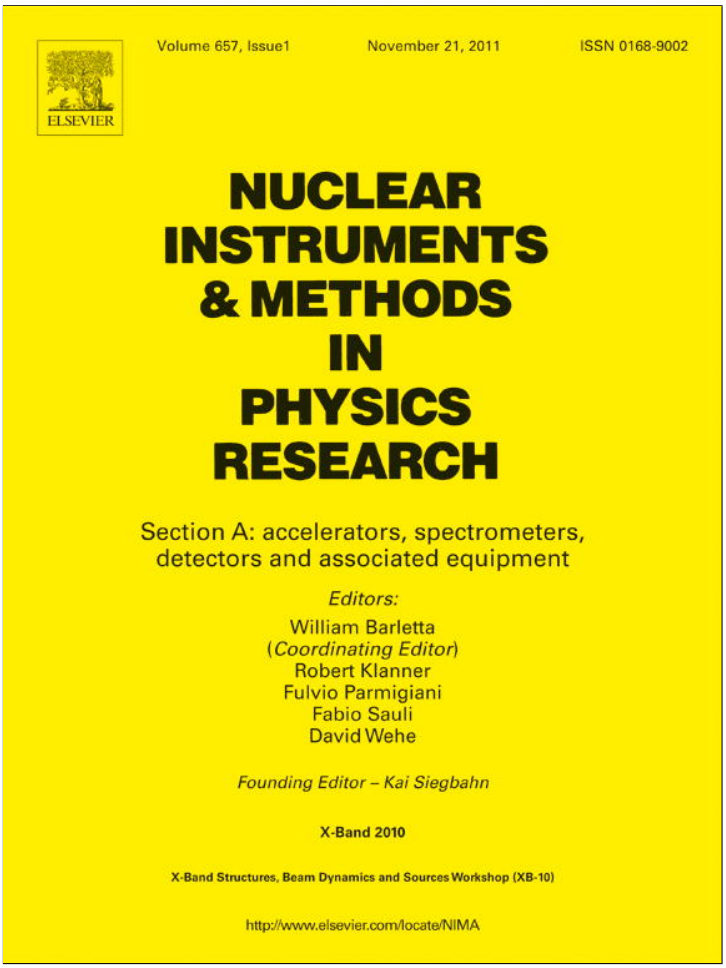

Nuclear Instruments and Methods in Physics Research A 657 (2011) 114–121

Contents lists available at ScienceDirect

Nuclear Instruments and Methods in Physics Research A

journal homepage: www.elsevier.com/locate/nima

Technological issues and high gradient test results on X-band molybdenum accelerating structures

B. Spataro [a,*], D. Alesini [a], V. Chimenti [a], V. Dolgashev [b], A. Haase [b], S.G. Tantawi [b], Y. Higashi [c], C. Marrelli [d], A. Mostacci [d], R. Parodi [e], A.D. Yeremian [b]

[a] INFN-LNF, Via E. Fermi 40, 00044 Frascati (RM), Italy
[b] SLAC, 2575 Sand Hill Road, Menlo Park, CA 94025,USA
[c] KEK 1-1 Oho, Tsukuba, Ibaraki, 305-0801 Japan
[d] University of Rome Sapienza, Department of Fundamental and Applied Science for Engineering, Via A. Scarpa 14, 00185 Rome, Italy
[e] INFN-Genova, Via Dodecaneso 33, 16146 Genova, Italy

ARTICLE INFO

Available online 7 June 2011

Keywords:
Linear accelerator
Particle acceleration
Resonators
Cavities
Amplifiers
Arrays
Rings

ABSTRACT

Two 11.424 GHz single cell standing wave accelerating structures have been fabricated for high gradient RF breakdown studies. Both are brazed structures: one made from copper and the other from sintered molybdenum bulk. The tests results are presented and compared to those of similar devices constructed at SLAC (*Stanford Linear Accelerator Center*) and KEK (*Kō Enerugī Kasokuki Kenkyū Kikō*). The technological issues to build both sections are discussed.

1. Introduction

The high gradient RF breakdown phenomena is still an open problem and dedicated research and development in this field has been launched within the linear-collider community in order to understand the breakdown mechanisms, which limit the high gradient performance [1].

The activity of designing, constructing and experimental testing of short 11.424 GHz high power standing wave (SW) sections began at INFN-LNF in the framework of a collaboration with SLAC and KEK laboratories [2]. The goal of the collaboration is to assess the maximum sustainable gradients in normal-conducting RF powered particle beam accelerators with extremely low breakdown probability. An intense technological activity is therefore committed to making X-band, accelerating structures, using different materials and methods [3–8]. Presently, the main processes under investigation are the following:

- high temperature brazing (800–1000) °C;
- soft bonding (250–300) °C;
- electroplating;
- molybdenum (Mo) sputtering on copper.

Single cell X-band standing wave structures operating at 11.424 GHz have been made with copper and sintered molybdenum bulk using a high temperature brazing procedure. High power tests for both structures have been conducted at SLAC. We report on the comparison of the breakdown rate probability in these two with structures of same geometry built at SLAC and KEK. The brazed Mo structure had a higher breakdown rate than the copper structures. We also report on the technological techniques for fabricating both structures and the possible effects that impacted the molybdenum brazed structure performance.

Issues concerning soft bonding, electroplating and molybdenum sputtering on copper techniques will be discussed in other papers.

2. Copper section construction and characterization

The device under study is a single cell in a 3-cell structure fed by a circular waveguide, as shown in Fig. 1. The central cell is the cell of interest and operates at high gradient, while the adjacent cells are used to match the RF power from the input circular waveguide and to balance the electric field in order to have the maximum intensity in the central one. This scheme is that used at SLAC to represent the performance a long accelerating structure composed of cells like the central cell in the test structure [9].

The π-mode accelerating electric field on axis and the reflection coefficient obtained from HFSS simulations [10] are shown in Fig. 2. They show a good match at the nominal RF frequency of $\sim$11.424 GHz and the maximum field intensity in the central cell doubles that of the adjacent cells.

The relevant cell dimensions for the copper structure are shown in the mechanical drawing in Fig. 3. The section has been made of oxygen free Cu (OFHC) using a numerical controlled

* Corresponding author.
E-mail address: bruno.spataro@lnf.infn.it (B. Spataro).

0168-9002/$ - see front matter © 2011 Elsevier B.V. All rights reserved.
doi:10.1016/j.nima.2011.05.020

lathe; each cell has been checked with a quality control test of the geometrical dimensions and the obtained machining precision is about ± 1.3 μm while the smoothness is about 70 nm The surface finishing was obtained directly by mechanical machining with custom cutting tools (diamond mono-crystal), avoiding any polishing technique. The machining was done at constant temperature (by means of a proper fluid) in order to maximize the uniformity of the mechanical dimension of the cells as much as possible. The standard cleaning procedure after the machining consists of two steps, the first with a 3% alkaline solution at 50 °C and the second with a 3% citric acid solution at 50 °C; each step is followed by a rinse first in tap water and then in distilled water. The pieces were dried in a dust free oven.

The brazing of the structure requires two different steps: the brazing of the copper–copper cells and the brazing of the stainless steel flanges on the copper beam pipe. Different composition of PALCUSIL (palladium–copper–silver) alloys with different melting points were used for the two different brazing procedures. In the subsequent brazing of the tuners one has to consider the effect of the gravitation; as shown in Fig. 3, they are placed in opposite sides of the structure and therefore they have been brazed in two different steps using the PALCUSIL alloy with decreasing melting temperature. After extensive tests, we have concluded that better brazing with PALCUSIL was obtained when the structure was brazed in vertical position since the presence of palladium in the alloy reduces the diffusion for capillarity.

We also investigated the brazing with CUSIL (copper–silver) alloy, resulting in optimal results for copper–copper brazing. To achieve the same high quality also for steel–copper brazing, the steel flanges were covered by a few μm layer of nickel or copper. The advantage of the CUSIL alloy is its independence from the whole structure orientation in the brazing oven.

The tuners are designed for plastic wall deformation, i.e. they are copper cylinders of 2.3 mm diameter acting on a copper surface 0.9 mm thick; the maximum allowed (measured) elastic deformation is of 0.6 mm height. Tuners are brazed in order to allow a push–pull tuning with a frequency dependence of 1.6 MHz/mm^3 of wall deformation. Each tuner by itself can recover the frequency shift due to mechanical machining tolerances and each cell is equipped with two tuners to double tuning range.

To identify structures we use abbreviations derived from the properties of the structure, the manufacturer and the serial number. As an example, the name 1C-SW-A5.65-T4.6-Cu-Frascati-#2 refers to a single standing wave high gradient cell (1C-SW) with a 5.65 mm

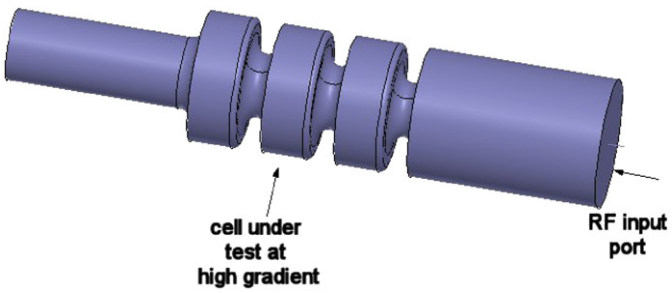

Fig. 1. Sketch of the cells structure to be tested at high power.

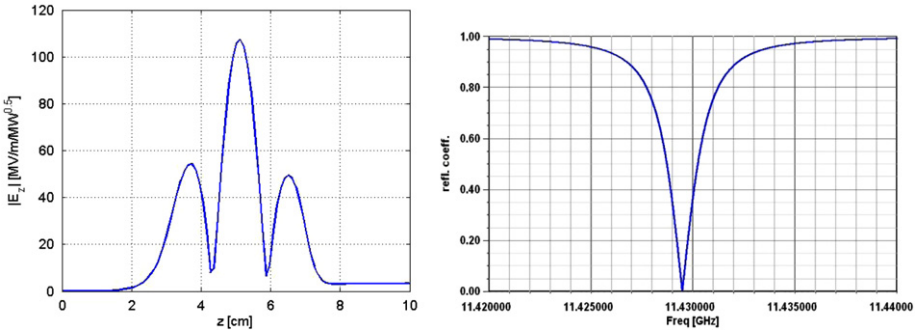

Fig. 2. Electric field profile on axis and reflection coefficient at the RF input port for the π-mode (HFSS simulations).

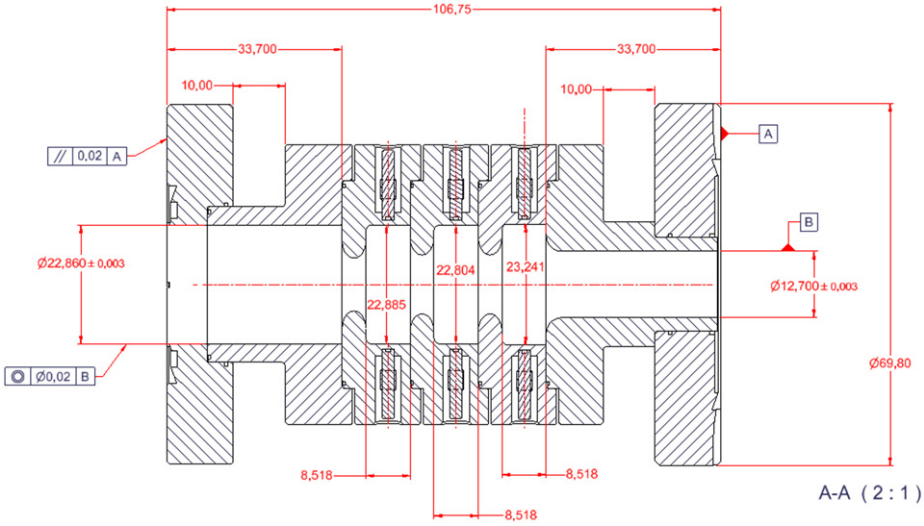

Fig. 3. Mechanical drawing of copper structure with dimensions.

aperture radius (A5.65) a 4.6 mm thick iris (T4.6) manufactured by INFN at the LNF. Finally, it is the second such structure manufactured at Frascati (#2).

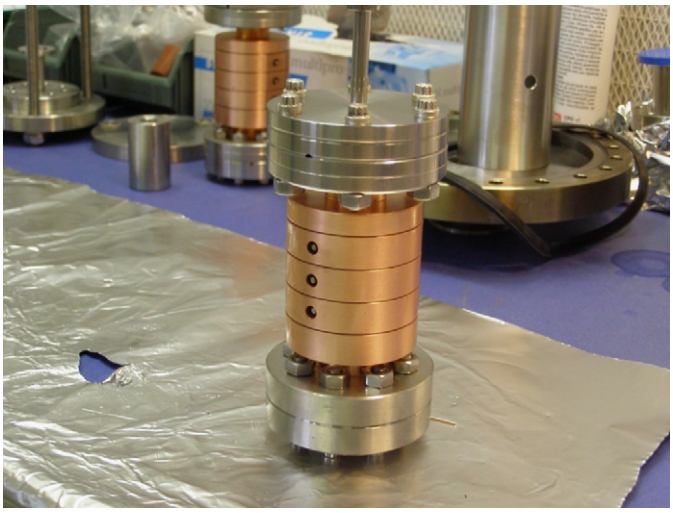

Fig. 4. Picture of the copper structure under test.

Table 1
Mode frequencies and quality factors (given by SUPERFISH) and measurement results of copper structure before brazing.

MODE	Res. Frequency [MHz] (simul.)	Res. Frequency [MHz] (meas.)	Quality factor (simul.)	Quality factor (meas.) [a]
1	10,980	10,983	8478	7700
2	11,118	11,127	8889	7600
3[b]	11,211	11,209	12,354	–
4	11,433	11,429	8380	7200

[a] After brazing the quality factors increase by ~5%.
[b] This mode is not a multi-cell mode but the mode of the circular waveguide. Its frequency is strongly depend on the circular waveguide length and strongly coupled with the probes used to characterize the other multi-cell modes.

3. Low power RF measurements results for the copper structure

Fig. 4 shows picture photograph of the copper structure designed according to Fig. 3. For the low power tests on the network analyzer, also known as cold tests, the structure has been closed at the ends by two metallic plates and two small probes have been inserted to excite the fields. With respect to the case of a circular mode launcher necessary for high power tests this configuration introduces a shift of the resonant frequencies and a perturbation of the electric field profile, but the perturbation on the π-mode is negligible. The multi-cell mode frequencies, quality factors and the related field profiles obtained by SUPERFISH [11] are reported in Table 1 and Fig. 5. The fourth mode corresponds to the π-mode.

The measured resonant frequencies and the quality factors of the structure before brazing are reported in Table 1 as well. As an example, the measured field profiles of the π-mode and the 0-mode (mode number 1) are reported in Fig. 6.

RF measurements after brazing show no significant differences from the cold tests.

4. Sintered molybdenum section

Sintered Mo is seen as a possible novel material for building accelerating sections with improved breakdown performances, because of its melting temperature higher than that copper.

It is not possible to wet stainless steel and sintered molybdenum bulk with PALCUSIL. A simple way to overcome this difficulty is to electrolytically deposit a thin layer (a few microns) of copper or nickel on the molybdenum. Then the eutectic Ag/Cu (silver–copper) alloy can be used without any difficulty because it wets very well both Cu and Ni.

A galvanoplastic process was adopted in order to obtain thin layers of Cu or Ni on Mo. A graphite anode was wrapped with a cotton pad that was soaked in a special electrolytic bath that contains Cu or Ni ions. This method is simple and quick and makes it easy to treat only the area of interest. The Cu layer is fixed on stainless steel or molybdenum through a vacuum thermal treatment at roughly 800 °C, before brazing, while the Ni layer needs no such treatment.

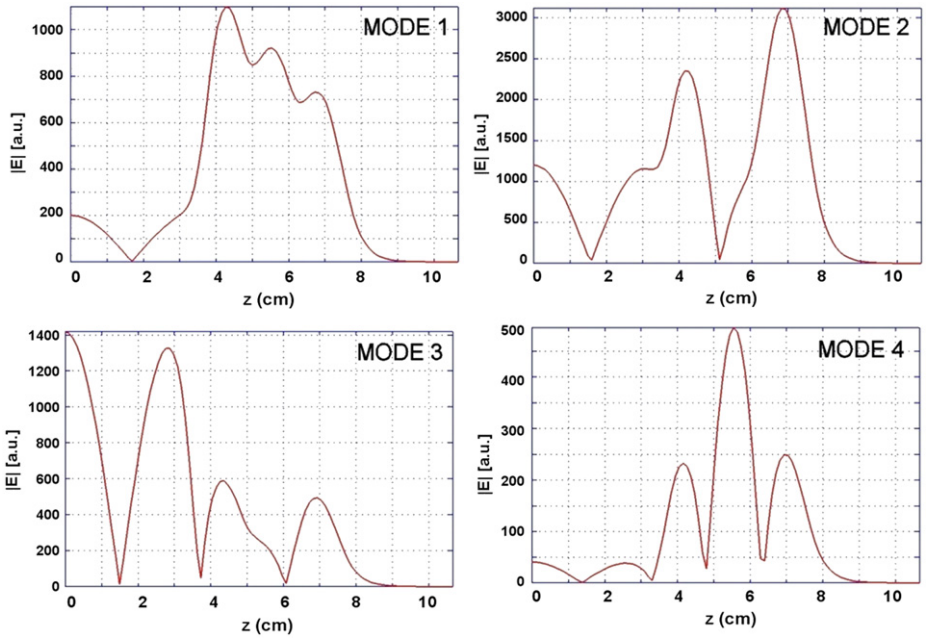

Fig. 5. Field profiles of the resonant modes (SUPERFISH results).

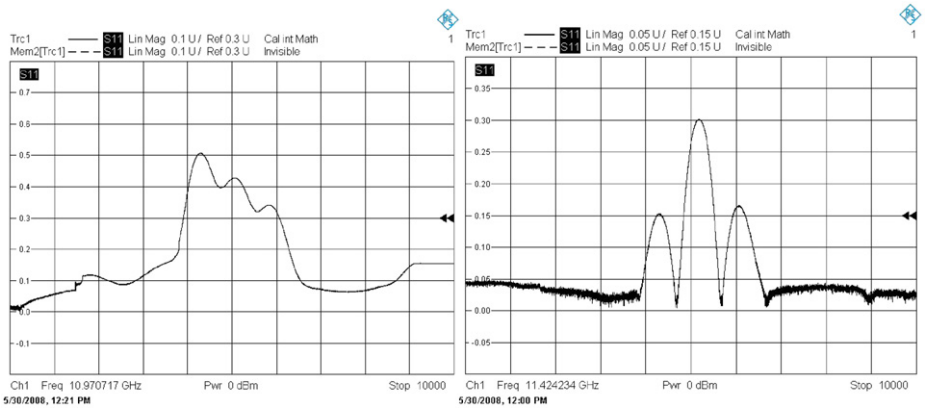

Fig. 6. Measured π-mode and 0-mode field profiles (by bead-pull technique) corresponding to MODE 1 and MODE 4 of Fig. 6, respectively.

Fig. 7. Picture of the molybdenum structure under test.

A 3 cells standing wave section made from sintered molybdenum bulk has been built and vacuum brazed following the above procedure (Fig. 7) using a Cu layer on the brazed surfaces. The Mo structure has slightly different dimensions than the Cu to compensate for the difference in surface conductivity [9], as shown in the mechanical drawing of Fig. 8.

The structure has been machined with a numerical controlled lathe with a ± 2.5 μm precision and smoothness better than 300 nm. The surface finishing was obtained directly by mechanical machining with custom tungsten carbide cutting tools. The tuners are identical to the copper case discussed in Section 2, except that the maximum plastic deformation is 0.3–0.4 mm in height on a 0.8 mm thick surface.

Low level RF measurements have been conducted before and after the brazing of the structure. The results after brazing are shown in Table 2, which compares the experimental results with simulations. The agreement is very good for the un-tuned structure. Field profiles measurements using the bead-pull technique gave similar results as for the copper structure.

5. High power RF test results on the copper and molybdenum brazed structure

The Cu and Mo brazed structures constructed at Frascati are of type 1C-SW-A5.65-T4.6. High power RF tests on both of these structures were conducted at SLAC. The results are shown in Figs. 9–12 where the breakdown rate as a function of the accelerating field in the central cavity of interest is reported for different pulse length. "All breakdown rate" refers to the total number of breakdowns, while "First breakdown rate" refers to the number of breakdown clusters. Breakdowns in the cluster occur one after another with klystron repetition frequency of 60 Hz. If the breakdowns are not in successive pulses they belong to different clusters. Typically there are 1–4 breakdowns in a cluster. We speculate that this number represents damage due to the first breakdown in the cluster. The "first breakdown rate" represents the characteristics of the breakdown trigger and "all breakdown rate" depends on both the trigger and the damage.

Fig. 9 shows the results related to the LNF Cu structure as a function of the accelerating gradient for different pulse length. Fig. 10 illustrates the comparison of the LNF Cu structure with similar Cu structures constructed in other laboratories as a function of the accelerating gradient and of the RF pulse length heating [12–14].

We note an excellent reproducibility of the results for the identical structures made in different laboratories.

The results for the Mo brazed structure are reported in Figs. 11 and 12. To our knowledge, this was the first systematic measurement of the breakdown rate for a totally molybdenum standing wave structure. From a comparison between Figs. 9 and 11 the results of the Mo brazed structure have the same trend than the Cu one. Although the material parameters (melting temperature, conductivity, etc.) are very different, the pulse length dependence of the breakdown rate is similar to copper structures having only a slight difference in the lowest breakdown gradient. For instance, in the case of 150 ns pulse length, the breakdown gradient in the brazed Mo structure is about 15% lower in respect to brazed Cu structure with similar first breakdown rate.

The right picture of Fig. 12 shows that molybdenum structure has extra pulsed heating as compared with the Cu structure [12–14].

6. Sintered molybdenum bulk brazed section internal inspection

After removing the brazed Mo structure from the high gradient test area, the structure was sectioned along the axis at the SLAC klystron laboratory for internal inspections. The structure was first split into 2 pieces using Electrical Discharge Machining (EDM). One of the half pieces was split again. On the initial sectioning, one of the molybdenum "extension tubes" broke adjacent to the stainless steel tube (SST) flange braze, as shown in Fig. 13.

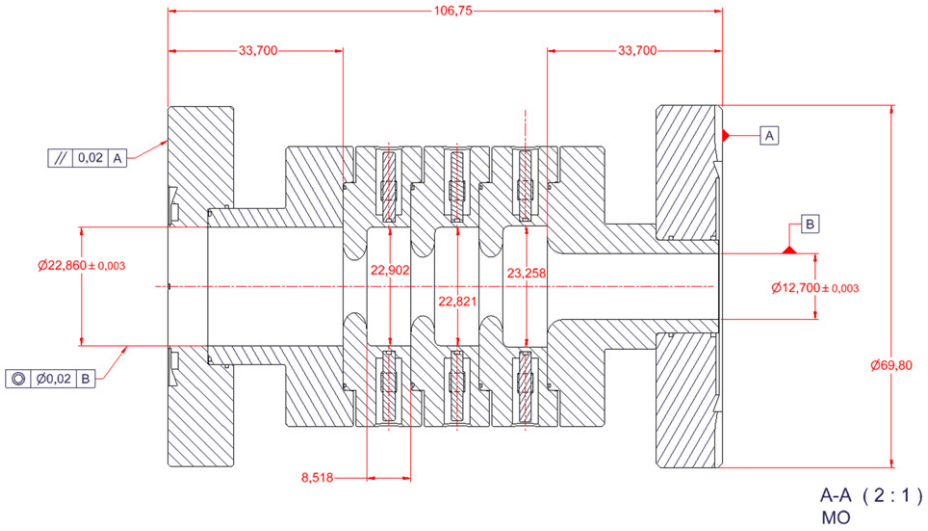

Fig. 8. Mechanical drawing of molybdenum structure with dimensions.

Table 2
Mode frequencies and quality factors (given by SUPERFISH) and measurement results of molybdenum structure after brazing.

MODE	Res. Frequency [MHz] (simul.)	Res. Frequency [MHz] (meas.)	Quality factor (simul.)	Quality factor (meas.)
1	10,985	10,977	4850	4850
2	11,120	11,129	5150	5000
3	11,430	11,425	4850	4800

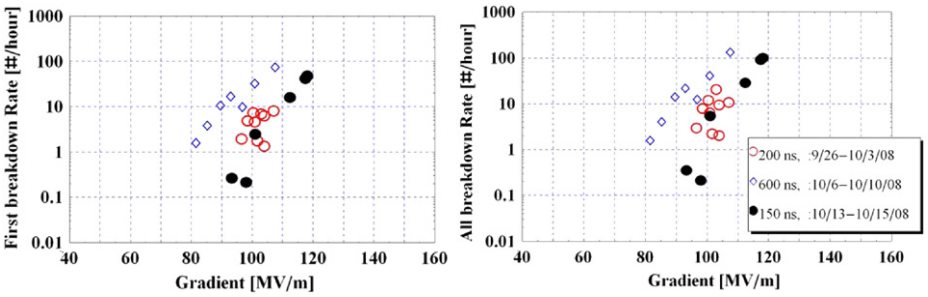

Fig. 9. Breakdown rate as a function of the accelerating gradient for different pulse length (brazed Cu Structure, 1C-SW-A5.65-T4.6-Cu-Frascati-#2).

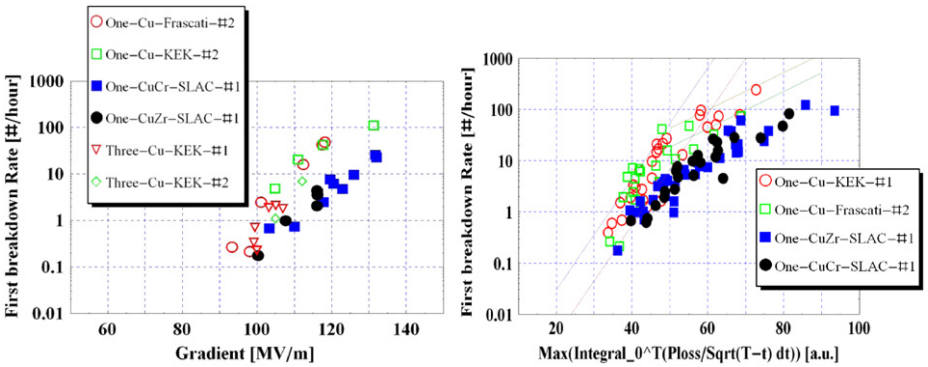

Fig. 10. Breakdown rate as a function of the accelerating gradient and of the peak pulse heating for the Cu-LNF structure compared with copper structures of same geometry, CuCr and CuZr structures of the same geometry and three-cell copper structures with same cell shape (the pulse length is 150 ns).

When one of the sections was cut again (again by EDM) both flanges on one of the pieces (a 1/4 section of the whole) detached as shown in Fig. 14. It appears that in the case where the joint failed in the braze area (see Fig. 14), the molybdenum cylinder wall was thick enough to withstand the differential expansion forces but that the braze joint was not. In the case of the other end, the thinner molybdenum wall was insufficient to withstand the forces applied (see Fig. 15). On closer inspection we found

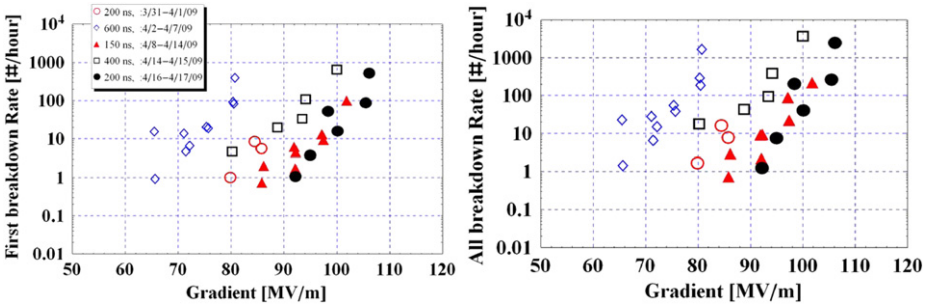

Fig. 11. Breakdown rate as a function of the accelerating gradient for different pulse length (Brazed Mo Structure), 1C-SW-A5.65-T4.6-Mo-Frascati-#1.

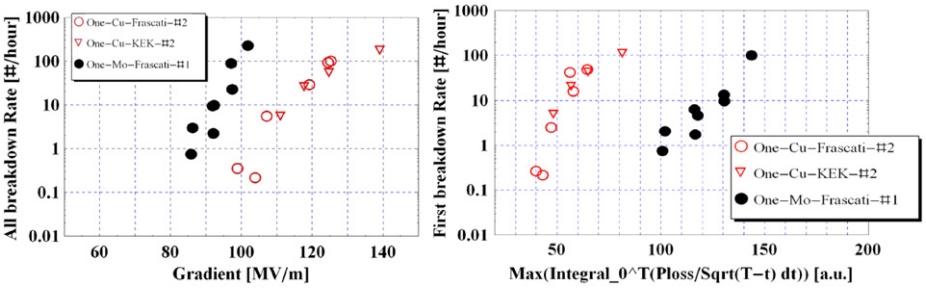

Fig. 12. Breakdown rate as a function of the accelerating gradient and the peak pulse heating for Mo-LNF structure compared with copper structures of same geometry (the pulse length is 150 ns).

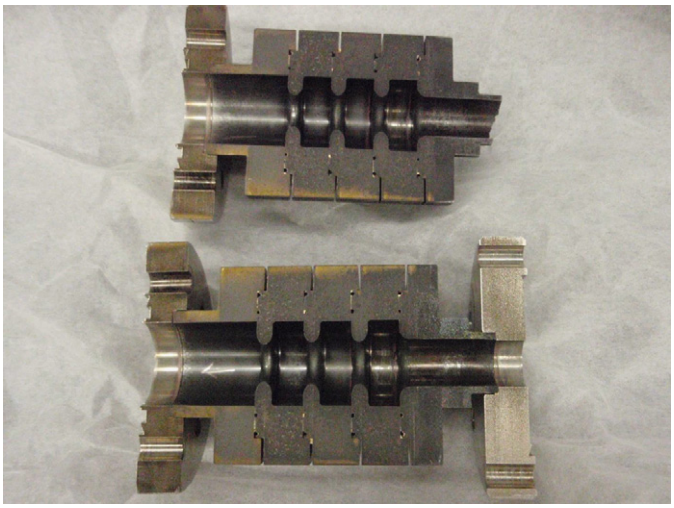

Fig. 13. Molybdenum structure was split up into 2 pieces using EDM.

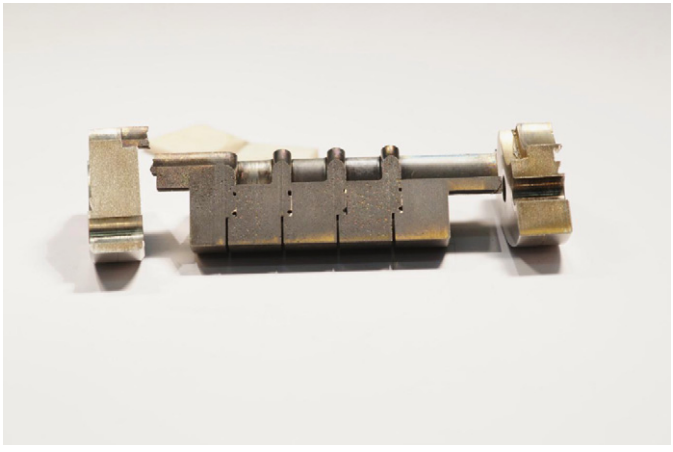

Fig. 14. When one of the sections was cut again (also by EDM) both flanges on one of the pieces (a 1/4 section of the whole) detached as shown.

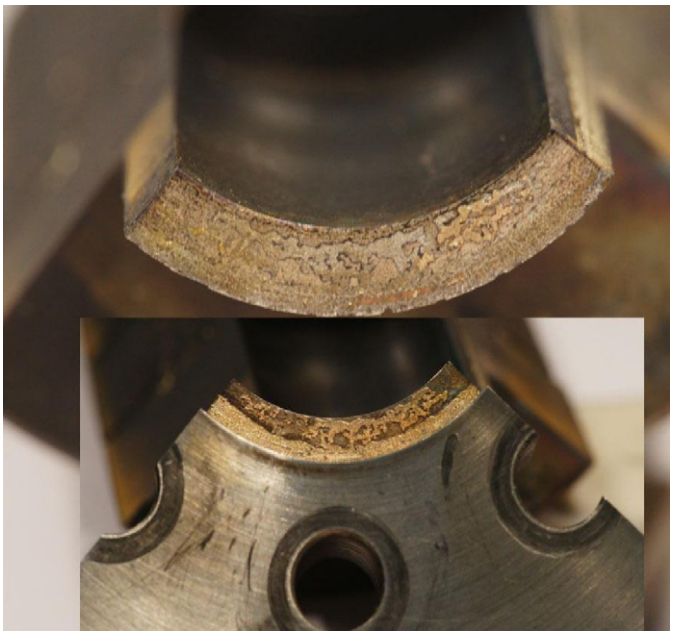

Fig. 15. Highlight of joint failed on the right side of Fig. 14.

that the joint was not completely filled with alloy, which would result in uneven loading and increased/concentrated stress. We think that this increased stress between the stainless steel and the molybdenum may have contributed to both failures. We speculate that during the braze cycle, a large radial gap between the stainless steel flange and molybdenum appeared due to larger thermal expansion of the stainless steel flange, which caused the non-uniform filling of the joint by the alloy (Fig. 16).

A possible solution that may reduce the stresses caused by the difference of thermal expansions could be to use an additional flexible part (in this case a thin-walled stain cylinder) between the molybdenum structure and stainless steel flange. This cylinder could be made from stainless steel, CuNi, or copper and it

should be properly designed to accommodate stresses created during the brazing. The joint between this flexible cylinder and molybdenum could be made with a groove that locks the outside diameter of the cylinder as shown on Fig. 17a. This joint has to be properly designed to have adequate clearance when the parts are heated during the brazing. The design should also take into account thermally induced forces between the locking grove and the cylinder. The joint can be strengthened by locking not only the outside diameter of the flexible cylinder, but also its inside diameter as shown on Fig. 17b. This, for example could be done for a flexible cylinder with large diameter.

We think that the joints between the structure cells could be improved by removing a void created by two contact surfaces on the iris side of the cell. This void is clearly visible in Fig. 18. The void could contribute to gas contamination and gas load during structure brazing and operation. For example, if inner contact surface has a vacuum leak and larger-diameter contact surface is vacuum tight, than this may create a virtual leak and adversely affect structure operation. By removing the second-larger-diameter contacting surface, we can improve the contact between the surfaces and avoid the uneven alloy filling of the joint seen on the zoomed part of Fig. 18.

Fig. 16. Highlight of molybdenum "extension tubes" failed adjacent to the SST flange on the left side of Fig. 14.

We suggest a joint consisting of a single set of mating faces 1–3 mm wide between the body and iris. We may also use "nested" cells by creating a cylindrical step of ~1.5 mm depth to lock the cells. The single mating surface will ensure contact at the cell–iris joint, would allow the cells to be made from much less material and may significantly reduce the potential for contamination and virtual leaks. A multi-step braze sequence can be used to facilitate the braze fillet control. In the noted design the first step would be a diffusion bond or an "alloy assisted" diffusion bond, if the body material and desired temperatures and pressures prevent direct bonding. Alloy assisted bonding uses temperature and pressure to create a bond between both sides of a filler (a thin "washer" in this case) and the base materials. If proper surface finishes, materials, temperatures and pressures are used the resulting bond should be leak tight with a well "filled" joint. The joint can then be brazed traditionally with a lower temperature alloy to provide additional strength.

We think that with a case of copper-diffusion-bond and secondary braze, the molybdenum can retain considerable hardness and strength. For example typical TZM (titanium zirconium molybdenum) stress relieving schedule would run to 980 °C and a full re-crystallization schedule may run above 1180 °C for over an hour.

7. Conclusions

Copper and Molybdenum X-band RF structures have been constructed at LNF using two different high temperature brazing techniques, one for each structure. The brazed Cu and Mo structures have been tested at high power at SLAC. The breakdown rates for

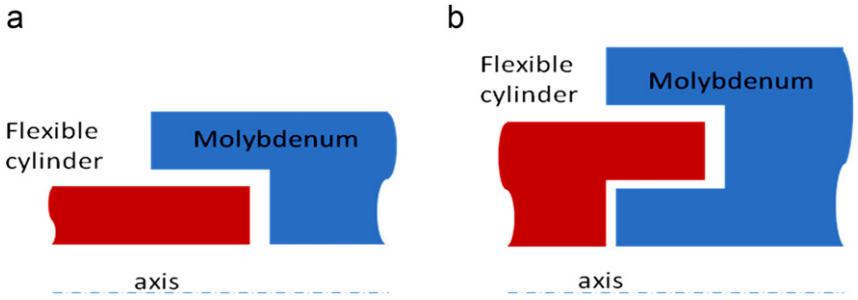

Fig. 17. (a and b) Possible joint designs between molybdenum and a flexible cylinder: (a) locking outside diameter of the flexible cylinder; (b) locking both inside and outside diameters of the flexible cylinder.

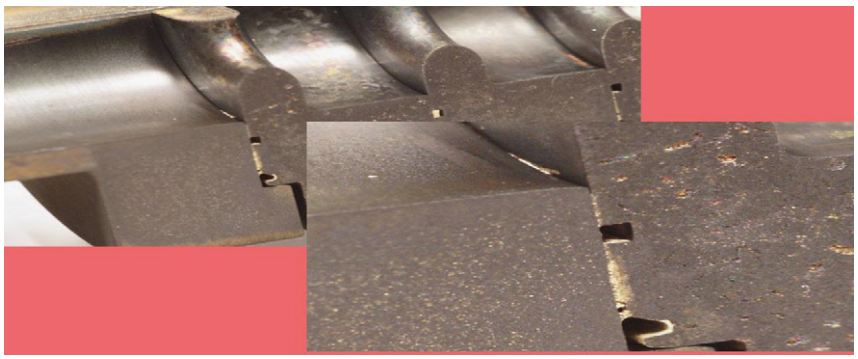

Fig. 18. The image highlights a body/iris joint typical of molybdenum structure.

the Cu structure are the same as those for similar structures constructed at SLAC and KEK. The breakdown rate of the brazed Mo structure is higher than that of coppers structure for same RF parameters. The main issues for sintered molybdenum bulk are the long time for machining the cavity, a 300 nm surface roughness using 'tungsten carbide' tools, the gas contamination and an uneven loading stress in the braze region. From the investigation of the sintered molybdenum bulk brazed section some technological problems have been detected and that information will be used to improve the performance of next brazed sintered Mo section.

Acknowledgments

The authors would like to acknowledge V. Lollo, P. Chimenti and R. Di Raddo for the helpful and precious contributions for designing and fabricating the sections.

References

[1] A. Grudiev, S. Calatroni, W. Wuensh, New local field quantity describing the high gradient limit of accelerating structures, PRST-Accelerators and Beams 12 (2009) 102001.
[2] V.A. Dolgashev, et al, Status of high power tests of normal conducting single-cell standing wave structures, in: Proceedings of the IPAC 2010, Kyoto, Japan, 2010, pp. 3810–3812 (and references therein).
[3] P. Chimenti, V. Chimenti, A. Clozza, R. Di Raddo, V. Lollo, M. Migliorati, B. Spataro, An Investigation on Electrforming Procedures for R.F. 11 GHz Linear Accelerating Structures at Frascati Laboratory, LNF–05/23 (IR), November 14, 2005.
[4] S.Bini, P. Chimenti, V. Chimenti, R. Di Raddo,V. Lollo, B. Spataro, F. Tazzioli, Electroforming Procedures Applied to the Construction of 11.4 GHz Linear Accelerating Structures: Status Report on SALAF Activity, RF-07/003, 29/05/2007.
[5] S. Bini, P. Chimenti, V. Chimenti, R. Di Raddo, V. Lollo, B. Spataro, F. Tazzioli, Status Report on SALAF Technical Activity on X-band Linear Accelerating Structures Project at Frascati Laboratories, SPARC-RF-08/001, July 31, 2008.
[6] S. Bini, P. Chimenti, V. Chimenti, R. Di Raddo, V.A.Dolgashev,V. Lollo, B. Spataro, Status Report on SALAF Technical Activity During the First Half of 2009, SPARC-RF-09/002 April 30, 2009.
[7] S. Bini, P. Chimenti, V. Chimenti, R. Di Raddo, V.A.Dolgashev,V. Lollo, B. Spataro, SALAF Group Technological Activity , SPARC-RF-09/003 June 30, 2009.
[8] S. Bini, P. Chimenti, V. Chimenti, R. Di Raddo, V.A. Dolgashev,Y. Higashi,V. Lollo, B. Spataro, Activities on the sputtered metals thin films for accelerating cavity applications, RF-10/001 12/01/10.
[9] V. Dolgashev, private communications and his seminar held at LNF, September 2010.
[10] 〈www.ansoft.com〉.
[11] J.H. Billen, L.M. Young, Particle Accelerator 7 (4) (1976) 213.
[12] V.A. Dolgashev, S.G. Tantawi, C.D. Nantista,Y. Higashi, T. Higo, Japan, RF Breakdown in Normal Conducting Single Cell Structures, SLAC-PUB-11707.
[13] O.A. Nezhevenko, On The Limitations of Accelerating Gradient in Linear Colliders Due to the Pulsed Heating, PAC97, Vancouver 1997, p. 3013.
[14] D.P. Pritzkau, RF Pulsed Heating, SLAC-Report-577, Ph.D. Dissertation, Stanford University, 2001.